

GEF-TH-4/1996
ETH-TH/96-08
hep-ph/yymmxxx

Constraints on the polarized gluon density in the proton from charm photoproduction

Stefano Frixione^a

ETH, Zürich, Switzerland

Giovanni Ridolfi

INFN, Sezione di Genova, Genoa, Italy.

Abstract

We consider the possibility of a direct determination of the polarized gluon density in the proton using charm production with polarized beams at HERA. We study total cross sections and distributions at leading order using different parametrizations of the polarized gluon density. We conclude that charm photoproduction data can be used to constrain the polarized gluon density in the proton if an integrated luminosity of 100 pb^{-1} will be achieved at HERA.

^a Work supported by the National Swiss Foundation

A direct measure of the spin-dependent gluon density in the proton, $\Delta g(x, Q^2)$, has never been performed (see ref. [1] for a recent review on polarized nucleon structure). Polarized deep inelastic scattering data allow to extract the structure function $g_1(x, Q^2)$ at different values of x and Q^2 and to obtain an indirect determination of Δg through scaling violation [2-5]. However, such indirect determinations are affected by large uncertainties, because of limited statistics and limited coverage of the x, Q^2 range of the presently available experimental data. On the other hand, a precise knowledge of the polarized gluon density is important in order to understand various aspects of the structure of polarized nucleons. For example, it has long been known [6, 7] that the anomalous gluon contribution to the first moment of g_1 , although formally of order α_s , does not vanish in the large- Q^2 limit, and therefore affects the extraction of the singlet axial charge from polarized deep inelastic scattering data. Furthermore, an independent determination of Δg would allow to test the reliability of the perturbative expansion, and to assess the importance of possible non-perturbative contributions.

In order to measure Δg directly, it is necessary to consider processes which are only or predominantly initiated by gluons; many have been studied in the past, like for example heavy quarkonia production in photon-gluon fusion [8], or the production of large- k_T jet pairs in deep-inelastic scattering [9,10]. Another interesting possibility is the production of heavy quarks in photon-proton collisions. This process has already been considered in refs. [11-13] in view of the possibilities of the electron-proton collider HERA, and the conclusion was reached that the study of total cross section asymmetries for heavy-quark photoproduction at HERA can be of little help in constraining the polarized gluon density in the proton. In this letter we reconsider this problem, in the light of recent experimental information on polarized deep inelastic scattering [14,15] and improved theoretical understanding, and of the planned values of luminosity for the HERA collider. We will also consider the impact of realistic experimental cuts on the observed quantities, and discuss some theoretical uncertainties. We will always refer to the production of charm quark-antiquark pairs, since this is the most favourable case for the kind of study we are considering here.

The electron-proton cross section for the production of heavy quarks can be reliably computed in the Weizsäcker-Williams approximation [16], where only the contribution of on-shell collinear photons radiated by the incoming electron beam is retained. Alternatively, the HERA experiments are capable to tag the scattered electron, thus determining the energy of the photon that initiated the reaction under

study. In this kind of analysis, HERA works as a photon-proton collider with a well defined photon energy, ranging between 70 and 270 GeV approximately. In both cases, the relevant parton subprocess at the leading order is

$$g(\hat{p}, \lambda_g) + \gamma(\hat{q}, \lambda_\gamma) \rightarrow c(k) + \bar{c}(k'), \quad (1)$$

where four momenta and helicities are indicated in brackets. The $\mathcal{O}(\alpha_{\text{em}}\alpha_s)$ partonic cross section for the process (1) is given by [11,12]

$$d\hat{\sigma}_{\gamma g}(\hat{s}, \hat{t}, \lambda_g, \lambda_\gamma) = \frac{e_c^2 \alpha_s}{16\hat{s}} [\Sigma + \lambda_g \lambda_\gamma \Delta] \beta d\cos\theta, \quad (2)$$

where

$$\Sigma = -\frac{8m^4 \hat{s}^2}{\hat{t}^2 \hat{u}^2} + 2 \frac{\hat{t}^2 + \hat{u}^2 + 4m^2 \hat{s}}{\hat{t} \hat{u}}, \quad (3)$$

$$\Delta = \frac{4m^2(\hat{t}^3 + \hat{u}^3)}{\hat{t}^2 \hat{u}^2} + 2 \frac{\hat{t}^2 + \hat{u}^2 - 2m^2 \hat{s}}{\hat{t} \hat{u}}, \quad (4)$$

m is the charm quark mass, e_c its electric charge, $\beta = \sqrt{1 - 4m^2/\hat{s}}$ and θ is the scattering angle in the γg center-of-mass frame. We have defined

$$\hat{s} = (\hat{p} + \hat{q})^2, \quad \hat{t} = (\hat{p} - k)^2 - m^2, \quad \hat{u} = (\hat{p} - k')^2 - m^2. \quad (5)$$

The quantity of interest is the difference

$$d\Delta\sigma_{\gamma p} = \frac{1}{2} (d\sigma_{\gamma p}^{\uparrow\uparrow} - d\sigma_{\gamma p}^{\uparrow\downarrow}), \quad (6)$$

where $d\sigma_{\gamma p}^{\uparrow\uparrow}$ and $d\sigma_{\gamma p}^{\uparrow\downarrow}$ are the differential cross sections for the $c\bar{c}$ photoproduction process, with parallel and antiparallel polarizations of the incoming photon and proton, respectively. In fact, it can be easily shown that at leading order the quantity in eq. (6) can be written as

$$d\Delta\sigma_{\gamma p}(s, t) = \Delta g(x_g, \mu_F^2) d\Delta\hat{\sigma}_{\gamma g}(\hat{s}, \hat{t}, \mu_R^2) dx_g, \quad (7)$$

where

$$\begin{aligned} d\Delta\hat{\sigma}_{\gamma g}(\hat{s}, \hat{t}) &= \frac{1}{4} \left(d\hat{\sigma}_{\gamma g}(\hat{s}, \hat{t}, +1, +1) + d\hat{\sigma}_{\gamma g}(\hat{s}, \hat{t}, -1, -1) \right. \\ &\quad \left. - d\hat{\sigma}_{\gamma g}(\hat{s}, \hat{t}, +1, -1) - d\hat{\sigma}_{\gamma g}(\hat{s}, \hat{t}, -1, +1) \right). \end{aligned} \quad (8)$$

In eq. (7) we defined $s = (p + \hat{q})^2$ and $t = (p - k)^2 - m^2$, where p is the four-momentum of the incoming proton, and x_g is the fraction of the proton longitudinal momentum carried by the gluon; μ_R and μ_F are the renormalization and factorization scales.

In the case of electroproduction, using the Weizsäcker-Williams approximation we have

$$d\Delta\sigma_{ep}(s, t) = \Delta f_{WW}(x_\gamma, Q_{WW}^2) \Delta g(x_g, \mu_F^2) d\Delta\hat{\sigma}_{\gamma g}(\hat{s}, \hat{t}, \mu_R^2) dx_g dx_\gamma, \quad (9)$$

where

$$\Delta f_{WW}(x_\gamma, Q_{WW}^2) = \frac{\alpha_{em}}{2\pi} \frac{1 - (1 - x_\gamma)^2}{x_\gamma} \log \frac{Q_{WW}^2 (1 - x_\gamma)}{m_e^2 x_\gamma^2}, \quad (10)$$

and we defined $s = (p + q)^2$, q being the electron four-momentum. The mass scale Q_{WW}^2 entering the Weizsäcker-Williams function has been chosen as discussed in ref. [17].

We will consider the three fits to Δg presented in ref. [3], which we will indicate with GS-A, GS-B, GS-C, and those presented in ref. [4], denoted by BFR-AB, BFR-OS and BFR-AR. The three parametrizations of Δg given in ref. [4] are obtained by performing fits to data within three different subtraction schemes for collinear divergences. Since a next-to-leading order calculation of the polarized partonic cross sections is not available, the scheme choice is immaterial in our analysis.

We begin by considering total cross sections. In the first row of table 1 we present (columns indicated with I) the total charm production cross section computed at next-to-leading order [18-20]. We show both the electroproduction results, obtained using the Weizsäcker-Williams approximation at the HERA center-of-mass energy of 314 GeV, and the photoproduction results, with a center-of-mass energy of the photon-proton system of 200 GeV. The factorization and renormalization scales are chosen equal to $2m$ and m respectively (see ref. [21] for a detailed discussion of scale choices).

We also show (columns II) the values of total cross sections with the conditions

$$p_T > 2 \text{ GeV} \quad (11)$$

$$|\eta| < 1.5, \quad (12)$$

imposed on the transverse momentum p_T and the pseudorapidity η of the observed heavy quark, (assuming that only one of the two heavy quarks produced is fully reconstructed). The conditions (11) and (12) approximately reproduce the present experimental situation of the HERA experiments. Finally, we show (columns III) the

	ep			γp		
	I	II	III	I	II	III
σ (NLO) (μb)	0.5505	0.09653	0.04542	3.929	0.9205	0.5268
$\Delta\sigma/\sigma$ $GS-A$	$7.19 \cdot 10^{-4}$	$5.66 \cdot 10^{-3}$	$9.58 \cdot 10^{-3}$	$2.78 \cdot 10^{-3}$	$1.87 \cdot 10^{-2}$	$2.82 \cdot 10^{-2}$
$\Delta\sigma/\sigma$ $GS-B$	$5.97 \cdot 10^{-4}$	$5.96 \cdot 10^{-3}$	$9.80 \cdot 10^{-3}$	$2.51 \cdot 10^{-3}$	$2.04 \cdot 10^{-2}$	$2.98 \cdot 10^{-2}$
$\Delta\sigma/\sigma$ $GS-C$	$3.87 \cdot 10^{-5}$	$3.56 \cdot 10^{-3}$	$5.41 \cdot 10^{-3}$	$3.38 \cdot 10^{-3}$	$1.34 \cdot 10^{-2}$	$1.79 \cdot 10^{-2}$
$\Delta\sigma/\sigma$ $BFR-AB$	$5.01 \cdot 10^{-4}$	$8.04 \cdot 10^{-3}$	$1.28 \cdot 10^{-2}$	$2.03 \cdot 10^{-3}$	$2.87 \cdot 10^{-2}$	$4.02 \cdot 10^{-2}$
$\Delta\sigma/\sigma$ $BFR-OS$	$5.71 \cdot 10^{-4}$	$5.56 \cdot 10^{-3}$	$9.20 \cdot 10^{-3}$	$2.24 \cdot 10^{-3}$	$1.91 \cdot 10^{-2}$	$2.79 \cdot 10^{-2}$
$\Delta\sigma/\sigma$ $BFR-AR$	$5.49 \cdot 10^{-4}$	$6.46 \cdot 10^{-3}$	$1.05 \cdot 10^{-2}$	$2.26 \cdot 10^{-3}$	$2.26 \cdot 10^{-2}$	$3.24 \cdot 10^{-2}$
$1/\sqrt{2\sigma\mathcal{L}}$	$9.53 \cdot 10^{-5}$	$2.28 \cdot 10^{-4}$	$3.32 \cdot 10^{-4}$	$2.77 \cdot 10^{-4}$	$5.73 \cdot 10^{-4}$	$7.57 \cdot 10^{-4}$

Table 1: *Total cross sections and total cross section asymmetries for $c\bar{c}$ production in ep collisions at $\sqrt{s_{ep}} = 314$ GeV and in γp collisions at $\sqrt{s_{\gamma p}} = 200$ GeV, for different choices of the polarized gluon density. The charm quark mass is 1.5 GeV, and the unpolarized gluon distribution is MRSA. The integrated luminosity for the ep system is 100 pb^{-1} .*

effect of applying the Peterson fragmentation function [22] to the produced charm quarks, in order to estimate the impact of hadronization phenomena. In columns III the cuts of eqs. (11) and (12) are still applied. Notice that in the absence of the cuts the total cross section values would be insensitive to fragmentation effects. On the other hand, the cuts introduce in the total cross section a dependence upon the p_T and η distributions; in particular, since Peterson fragmentation softens the p_T spectrum, the low- p_T region gives a contribution to the cross section larger than in the bare quark case. This explains the lower values of columns III with respect to columns II.

In the following six rows we display the values of the asymmetry $\Delta\sigma/\sigma$ in the same cases, obtained with the six different parametrizations of Δg . It must be stressed that the unpolarized cross section σ that appears in the denominator of the asymmetry is computed at the leading order, because a next-to-leading order calculation for the polarized cross section is not available. However, one might expect that the effect of radiative corrections approximately cancels in the ratio $\Delta\sigma/\sigma$. Notice that the asymmetries obtained with the fragmented quarks are larger than those for bare quarks, at variance with the case of the total cross sections. This is due to the fact that the dominant contribution to $\Delta\sigma/\sigma$ is given by the large- p_T region, where the asymmetry values are larger for fragmented quarks than for bare ones. We will discuss

again this issue when dealing with differential cross sections.

The next-to-leading order value of σ can then be used to estimate the sensitivity of the experiment. A rough estimate of the minimum value of the asymmetry observable at HERA can be obtained by requiring the difference between the numbers of events with parallel and antiparallel polarizations of the initial state particles to be larger than the statistical error on the total number of observed events. This gives

$$\left[\frac{\Delta\sigma}{\sigma}\right]_{min} \simeq \frac{1}{\sqrt{2\sigma\mathcal{L}\epsilon}}, \quad (13)$$

where \mathcal{L} is the integrated luminosity and the factor ϵ accounts for the experimental efficiency for charm identification and the fact that the initial beams are not completely polarized. The values of $1/\sqrt{2\sigma\mathcal{L}}$ in the various cases are given in the last row of table 1, for $\mathcal{L} = 100 \text{ pb}^{-1}$. In the case of photoproduction, the effective luminosity has been estimated by assuming that the results obtained with photons such that $170 \text{ GeV} < \sqrt{s_{\gamma p}} < 230 \text{ GeV}$ can be reliably described by the cross section for an incoming monochromatic photon with $\sqrt{s_{\gamma p}} = 200 \text{ GeV}$. The ep luminosity of 100 pb^{-1} has then been rescaled by a factor equal to the integral of the Weizsäcker-Williams function in the appropriate range.

By inspection of table 1, we conclude that the asymmetries of practical interest (columns II and III) are always larger than the corresponding minimum observable values with an integrated luminosity of 100 pb^{-1} even if an experimental efficiency of 1% is assumed. We also observe that the asymmetry is generally larger in the phase space region defined by eqs. (11) and (12). In practice, the quantity $\mathcal{L}\Delta\sigma$ is required to be larger than 5 or 10 events, in order to distinguish the signal from the background. This condition appears to be fulfilled for all the cases considered in table 1, with $\mathcal{L} = 100^{-1}$. We also observe that all the chosen parametrizations for the polarized gluon density give similar results for the total cross section asymmetry. It seems therefore difficult to distinguish among them with this kind of measurement.

We now turn to differential distributions. From table 1 we know that the asymmetry tends to become larger in the phase-space region where the conditions (11) and (12) are satisfied; we will therefore present our predictions with the kinematical cuts (11) and (12) applied. We will consider only the GS-A and BFR-AB parametrizations.

In fig. 1 we show the asymmetry versus the transverse momentum of the observed quark for ep collision at a center-of-mass energy of 314 GeV. The scale choice is $\mu_R = \mu_0$, $\mu_F = 2\mu_0$, with $\mu_0 = \sqrt{p_T^2 + m^2}$. As previously observed, the asymmetry

increases with increasing transverse momentum. Observe also that the asymmetry for fragmented quarks is always larger than that for bare quarks over the whole p_T range considered, consistently with the analogous behaviour of total cross sections. The results obtained with the two parametrizations for Δg are quite close to each other, although they display slightly different shapes: the BFR parametrization produces larger asymmetries in the low- p_T region. The effect of Peterson fragmentation on

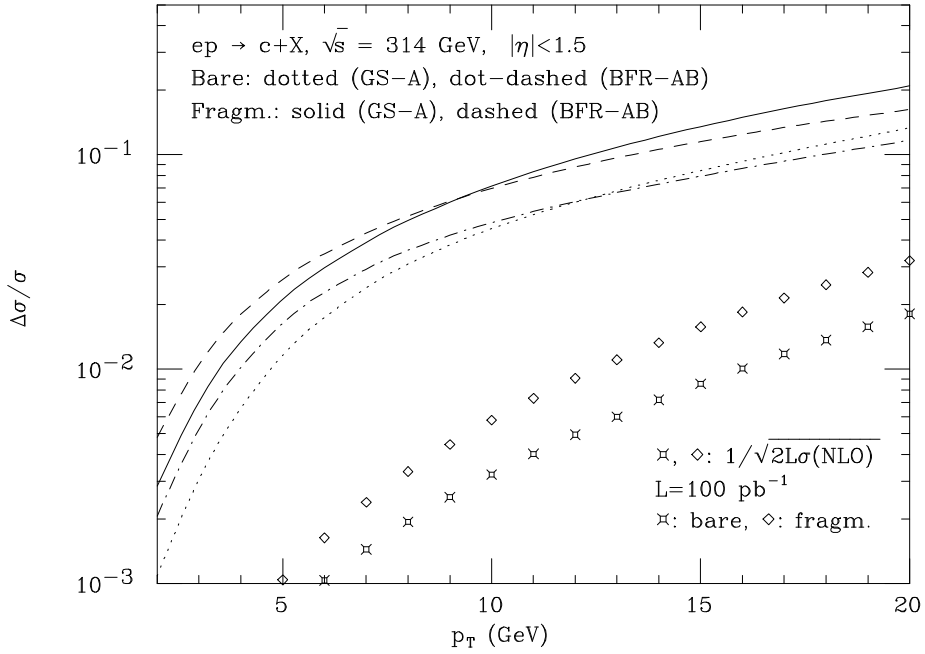


Figure 1: *Asymmetry cross section versus transverse momentum in ep collisions at $\sqrt{s} = 314$ GeV. The minimum observable asymmetry, computed at next-to-leading order, is also displayed.*

the shape of this distribution is very small. In fig. 1 we also show the quantity defined in eq. (13) for $\epsilon = 1$ and $\mathcal{L} = 100 \text{ pb}^{-1}$, as an indication for the minimum observable value of the asymmetry. In this case, the quantity σ appearing in the RHS of eq. (13) is the next-to-leading order cross section for a given p_T bin. We used a bin size of 1 GeV; clearly, a larger bin size would decrease the minimum observable asymmetry; on the other hand, by enlarging the bins the resolution of the measurement would get worse. From fig. 1, we can see that there exists a wide p_T region where the predicted asymmetries are more than one order of magnitude above the corresponding minimum observable asymmetry. Furthermore, the value of

the asymmetry for p_T above 10 GeV is of the order of few tens of percent. We can

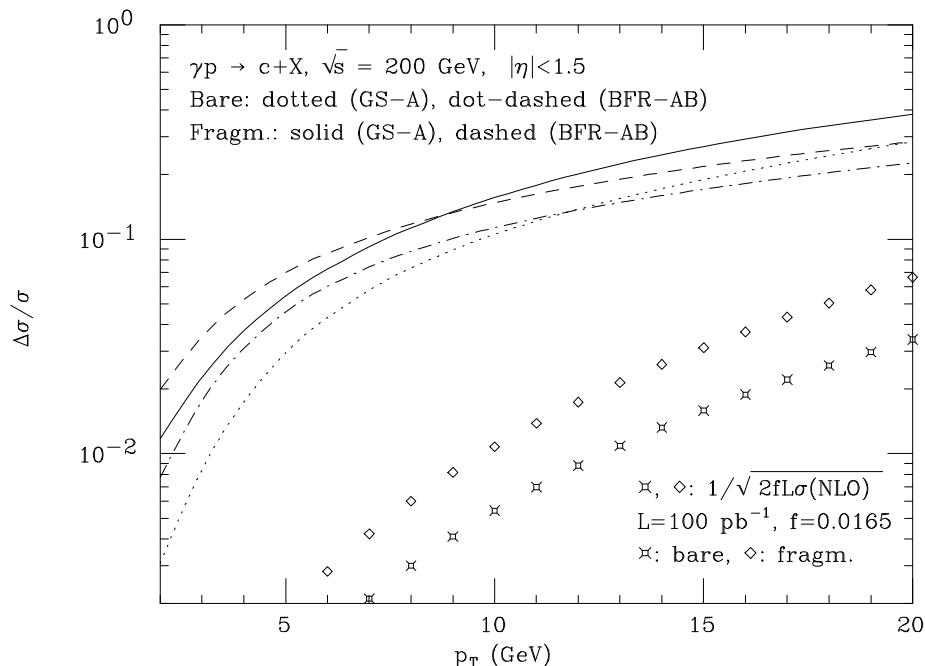


Figure 2: *Asymmetry cross section versus transverse momentum in γp collisions at $\sqrt{s} = 200$ GeV. The minimum observable asymmetry, computed at next-to-leading order, is also displayed.*

therefore conclude that the p_T distribution could be used to extract information on the polarized gluon density, even with a low experimental efficiency. The shape of the distribution could in principle provide with the possibility of discriminating among the various sets for Δg . However, since the predictions for different sets are quite close to each other, this kind of measurement does not appear to be feasible with the planned luminosity values.

Figure 2 is the analogous of fig. 1 for γp collisions at a center-of-mass energy of 200 GeV. The asymmetry values turn out to be larger than for ep collisions in the whole p_T range, and the curves appear to be slightly flatter than in the previous case. On the other hand, the minimum observable value is larger than before. We computed the effective luminosity for the incoming photon as in the case of total cross sections.

It is also interesting to consider fully exclusive distributions, despite the fact that a large statistics is needed in order to reconstruct completely both the produced charm

and anti-charm. In analogy with the unpolarized case (see ref. [23]), we can rewrite eq. (9) as

$$\frac{d\Delta\sigma_{ep}}{dy_{c\bar{c}}dM_{c\bar{c}}^2} = \frac{1}{s}\Delta f_{WW}(x_\gamma, Q_{WW}^2)\Delta g(x_g, \mu_F^2)\Delta\hat{\sigma}_{\gamma g}(M_{c\bar{c}}^2), \quad (14)$$

with

$$x_\gamma = \frac{M_{c\bar{c}}}{\sqrt{s}}\exp(-y_{c\bar{c}}), \quad (15)$$

$$x_g = \frac{M_{c\bar{c}}}{\sqrt{s}}\exp(y_{c\bar{c}}). \quad (16)$$

In eqs. (14), (15) and (16) $M_{c\bar{c}}^2 = \hat{s}$ is the invariant mass of the $c\bar{c}$ pair, and $y_{c\bar{c}}$ its rapidity in the electron-proton center-of-mass frame. We have positive rapidities in

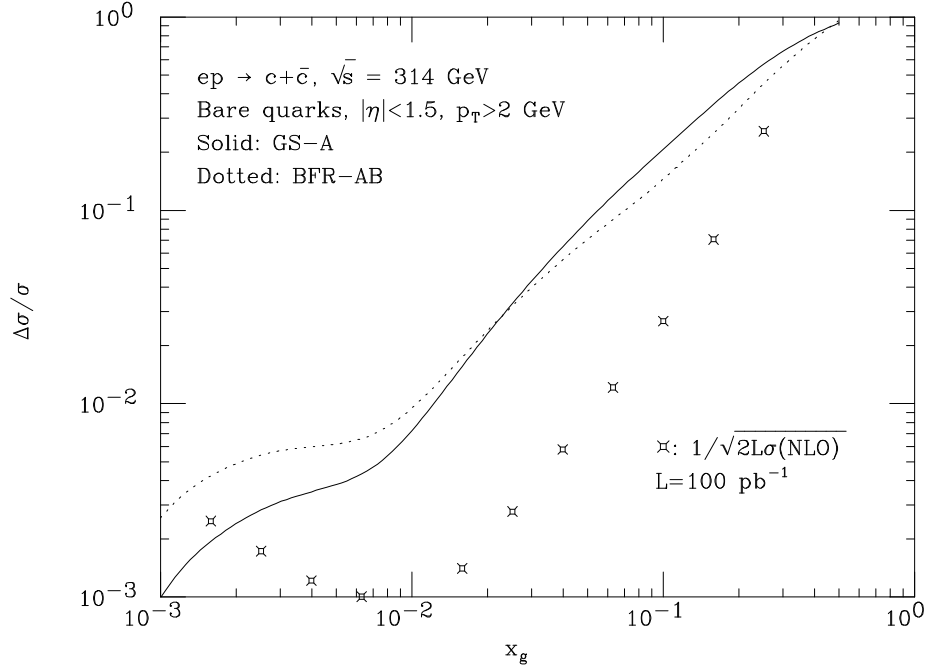


Figure 3: *Asymmetry cross section versus x_g in ep collisions at $\sqrt{s_{ep}} = 314$ GeV. The minimum observable asymmetry, computed at next-to-leading order, is also displayed.*

the proton direction. Identifying the LHS of eq. (14) with the experimental data, we can invert this equation to get

$$\Delta g(x_g, \mu_F^2) = \frac{s}{\Delta f_{WW}(x_\gamma, Q_{WW}^2)\Delta\hat{\sigma}_{\gamma g}(M_{c\bar{c}}^2)} \left(\frac{d\Delta\sigma_{ep}}{dy_{c\bar{c}}dM_{c\bar{c}}^2} \right)^{data}. \quad (17)$$

We present our results directly in terms of the variable x_g , exploiting the identity

$$\frac{d\Delta\sigma_{ep}}{dy_{c\bar{c}}dM_{c\bar{c}}^2} = x_g \frac{d\Delta\sigma_{ep}}{dx_g dM_{c\bar{c}}^2}. \quad (18)$$

In fig. 3 we show our predictions for the x_g asymmetry in ep collisions at a center-of-mass energy of 314 GeV. In this case, the reference scale μ_0 is equal to $\sqrt{(p_{cT}^2 + p_{\bar{c}T}^2)/2 + m^2}$. We do not present the result for the fragmented quarks. In fact, when Peterson fragmentation is applied, x_g is not expressed in terms of the invariant mass and rapidity of the pair as in eq. (16). The correct relationship could in principle be worked out, but it is more straightforward to obtain the $c\bar{c}$ cross section by directly performing the deconvolution on the measured cross section for charmed hadron production. This procedure can be applied using different hadronization models, thus obtaining an estimate of the dependence of the result upon the assumed hadronization mechanism.

By inspection of fig. 3, we can conclude that the polarized gluon density can be probed with a good resolution (we used a bin size of 0.2 in the variable $\log x_g$) in the range $(10^{-2}, 10^{-1})$, if the experimental efficiency is not too small. The GS-A and BFR-AB results are quite similar, and it appears unlikely that this kind of measurement could discriminate between them.

In this paper we have studied the problem of measuring the polarized gluon density in the proton using the charm data which will be collected at the HERA collider in the polarized configuration. We used a leading-order QCD calculation, since the polarized short distance partonic cross sections are not available at the next-to-leading order. For this reason, we presented our results in terms of asymmetries, which are more likely to be stable under radiative corrections than the polarized or unpolarized cross sections. We have shown that, assuming an integrated luminosity of 100 pb^{-1} , the total cross section asymmetries can be measured even with a very low experimental efficiency. The measurement of single-inclusive and double-differential distributions also appears to be feasible, although in the latter case a higher luminosity is certainly needed. With a luminosity of 100 pb^{-1} , it seems difficult to distinguish among the various parametrizations for the polarized gluon density.

We have not considered the inclusion of the hadronic component of the photon, which is known to be important in the HERA regime. Unfortunately, no information on the polarized parton densities in the photon is available up to now, and therefore no theoretical estimate can be given. It is known [24] that the p_T spectrum of the hadronic component is softer than the pointlike one in the unpolarized case, and

therefore the cut of eq. (11) reduces the impact of the hadronic component on the full unpolarized results. This might not happen in the polarized case. However, for hadronic photons a sizeable fraction of the photon momentum is lost into hadronic fragments, that can be observed in the photon direction. In this way it should be possible to disentangle the hadronic component from the pointlike one.

Acknowledgements

We wish to thank S. Forte, C. Grab, P. Nason and L. Rolandi for useful suggestions.

References

- [1] S. Forte, Proceedings of the 6th International Conference on Elastic and Diffractive Scattering, Blois, France, 20-24 Jun 1995, preprint CERN-TH-95-305, hep-ph/9511345;
G. Altarelli, Proceedings of the International School of Subnuclear Physics, Erice, 1989, preprint CERN-TH-5675-90.
- [2] R.D. Ball, S. Forte and G. Ridolfi, *Nucl. Phys.* **B444**(1995)287.
- [3] T. Gehrmann and W.J. Stirling, preprint DTP/95/82, hep-ph/9512406, to appear in *Phys. Rev. D*.
- [4] R.D. Ball, S. Forte and G. Ridolfi, hep-ph/9510449, to appear in *Phys. Lett. B*.
- [5] M. Gluck, E. Reya, M. Stratmann and W. Vogelsang, preprint DO-TH-95-13, hep-ph/950834, to appear in *Phys. Rev. D*.
- [6] G. Altarelli and G.G. Ross, *Phys. Lett.* **B212**(1988)391.
- [7] G. Altarelli and B. Lampe, *Z. Phys.* **C47**(1990)315.
- [8] J.-P. Guillet, *Z. Phys.* **C39**(1988)75.
- [9] G. Altarelli and W.J. Stirling, *Particle World* **1**(1989)40.
- [10] R.D. Carlitz, J.C. Collins and A.H. Mueller, *Phys. Lett.* **B214**(1988)229.
- [11] M. Glück and E. Reya, *Z. Phys.* **C39**(1988)569.
- [12] M. Glück, E. Reya and W. Vogelsang, *Nucl. Phys.* **B351**(1991)579.
- [13] W. Vogelsang, in *Physics at HERA, Proc. of the Workshop Vol. 1*, eds. W. Büchmüller and G. Ingelman (1991).
- [14] D. Adams et al., SMC Collaboration, *Phys. Lett.* **B329**(1994)399;
Phys. Lett. **B357**(1995)248.
- [15] K. Abe et al., E143 Collaboration, *Phys. Rev. Lett.* **74**(1995)346;
Phys. Rev. Lett. **75**(1995)25.

- [16] C.F. Weizsäcker, *Z. Phys.* **88**(1934)612;
E.J. Williams, *Phys. Rev.* **45**(1934)729.
- [17] S. Frixione, M.L. Mangano, P. Nason and G. Ridolfi, *Phys. Lett.* **B319**(1993)339.
- [18] R.K. Ellis and P. Nason, *Nucl. Phys.* **B312**(1989)551.
- [19] J. Smith and W.L. van Neerven, *Nucl. Phys.* **B374**(1992)36.
- [20] S. Frixione, M.L. Mangano, P. Nason and G. Ridolfi, *Phys. Lett.* **B348**(1995)633.
- [21] S. Frixione, M.L. Mangano, P. Nason and G. Ridolfi, *Nucl. Phys.* **B412**(1994)225.
- [22] C. Peterson, D. Schlatter, I. Schmitt and P. Zerwas, *Phys. Rev.* **D27**(1983)105.
- [23] S. Frixione, M.L. Mangano, P. Nason and G. Ridolfi, *Phys. Lett.* **B308**(1993)137.
- [24] S. Frixione, P. Nason and G. Ridolfi, *Nucl. Phys.* **B454**(1995)3.